PALEOCEANOGRAPHY, VOL. 28, 377–387, doi:10.1002/palo.20035, 2013

Comparison of organic ($U^{K'}_{37}$, TEX^{H}_{86}, LDI) and faunal proxies (foraminiferal assemblages) for reconstruction of late Quaternary sea surface temperature variability from offshore southeastern Australia

Raquel A. Lopes dos Santos,[1,2] Michelle I. Spooner,[3,4] Timothy T. Barrows,[5] Patrick De Deckker,[3] Jaap S. Sinninghe Damsté,[1] and Stefan Schouten[1]

Received 13 June 2012; revised 25 March 2013; accepted 13 June 2013; published 2 August 2013.

[1] Several proxies have been developed to reconstruct past sea surface temperature (SST), but different proxies may reflect temperatures of different seasons and each proxy is characterized by certain uncertainties. Therefore, a multiproxy approach is preferred to precisely reconstruct SST. Here, we reconstruct SST of the ocean offshore southeastern Australia (Murray Canyons area) for the last ~135 ka using three independent organic proxies (TEX^{H}_{86} based on glycerol dialkyl glycerol tetraethers (GDGTs), $U^{K'}_{37}$ based on alkenones, and LDI based on long-chain diols) in addition to foraminiferal faunal assemblages. The organic proxy records show similar trends, with the highest temperature (21°C for $U^{K'}_{37}$ and TEX^{H}_{86}, and 25°C for LDI) during the last interglacial and lowest temperature (8°C for TEX^{H}_{86}, 10°C for $U^{K'}_{37}$, and 12°C for LDI) during the Last Glacial Maximum. However, the differences in absolute SST estimates obtained by the organic proxies varied over time with differences of up to 9°C between LDI and TEX^{H}_{86}. The seasonal SST reconstructions based on the modern analogue of foraminiferal assemblages also show similar trends as the organic proxies with highest temperatures during the last interglacial (23°C for the warmest month SST, 20°C for mean annual, and 18°C for the coolest month) and lowest temperature during the Last Glacial Maximum (14°C for the warmest month, 11°C for mean annual, and 9°C for the coolest month). Down core comparison between the reconstructed SSTs of the organic and inorganic proxies shows that LDI-inferred temperatures compare well with the temperature of the warmest month, TEX^{H}_{86} with the temperature of the coolest month, and $U^{K'}_{37}$ with mean annual temperature. An increase in TEX^{H}_{86} SST estimates relative to those of other proxies during deglaciations and interglacials suggests that either winter temperatures rapidly warmed, possibly due to an invigoration of the Leeuwin Current over the core site, or there was a change in the growth season of the Thaumarchaeota, the source organism of GDGTs. Our study shows the benefits of a multiproxy approach in the interpretation of SST proxies, leading to a more robust knowledge of past ocean temperature changes.

Citation: Lopes dos Santos, R. A., M. I. Spooner, T. T. Barrows, P. De Deckker, J. S. Sinninghe Damsté, and S. Schouten (2013), Comparison of organic ($U^{K'}_{37}$, TEX^{H}_{86}, LDI) and faunal proxies (foraminiferal assemblages) for reconstruction of late Quaternary sea surface temperature variability from offshore southeastern Australia, *Paleoceanography*, *28*, 377–387, doi:10.1002/palo.20035.

Additional supporting information may be found in the online version of this article.

[1]Department of Marine Organic Biogeochemistry, NIOZ Royal Netherlands Institute for Sea Research, Den Burg, Netherlands.
[2]Now at British Geological Survey, Nottingham, UK.
[3]Research School of Earth Sciences, Australian National University, Canberra, ACT, Australia.
[4]Now at Planet Gas Limited, Sydney, New South Wales, Australia.
[5]Geography, College of Life and Environmental Sciences, University of Exeter, Exeter, UK.

Corresponding author: R. A. Lopes dos Santos, British Geological Survey, Nicker Hill, Keyworth, Nottingham NG12 5GG, UK. (raquel@bgs.ac.uk)

0883-8305/13/10.1002/palo.20035

1. Introduction

[2] Accurate estimation of sea surface temperature (SST) from low- to high-latitude environments is a primary objective for paleoceanographic studies since SST is a crucial element of global climate. Several proxies have been used to reconstruct SST and are either based on inorganic (shells or skeletons) or organic (lipids) fossil remains. Both types of proxies have different uncertainties associated with them, and therefore, a multiproxy approach is often used to constrain these uncertainties. An approach used in the past has been the use of oxygen isotope composition of planktonic foraminifera tests to estimate temperature [*Urey*, 1947;

Fischer and Wefer, 1999, and references cited therein]. However, other factors such as ice volume [e.g., *Lea et al*., 2002, and references cited therein], the state of preservation of the tests [e.g., *Pearson et al*., 2001], species-dependent vital effects as well as seawater composition, such as carbonate ion concentration and salinity [e.g., *Spero et al*., 1997], influence the $\delta^{18}O$ values of carbonates. Another common technique is based on the analysis of fossil species assemblages [*Imbrie and Kipp*, 1971; *Hutson*, 1977; *Pflaumann et al*., 1996; *Malmgren and Nordlund*, 1997; *Waelbroeck et al*., 1998], but estimates based on this approach can be compromised by selective dissolution and lack of modern analogues [*Barrows and Juggins*, 2005]. In addition, planktonic foraminiferal assemblages can reflect environmental variables other than sea surface temperature, and transfer function approaches have also been used to assess thermocline depth [*Andreasen and Ravelo*, 1997], mixed layer depth [*Spooner et al*., 2005], and productivity [*Mix*, 1989]. The Mg/Ca ratios of planktonic foraminifera have also been shown to be a useful proxy for SST reconstructions [*Nürnberg et al*., 1996]. However, these ratios can also be affected by carbonate ion concentration [e.g., *Elderfield et al*., 2006], pH [*Lea et al*., 1999], salinity [*Lea et al*., 2002; *Ferguson et al*., 2008], species-dependent vital effects [e.g., *Eggins et al*., 2004], and test dissolution [*Brown and Elderfield*, 1996]. All these proxies have been used to reconstruct mean annual SST, but studies have shown that they sometimes better record a seasonal or a subsurface temperature [e.g., *Spooner et al*., 2011; *Haarmann et al*., 2011].

[3] The main advantage of organic proxies for paleothermometry in comparison to inorganic ones is that they are not substantially influenced by the elemental and isotopic composition of sea water. The first organic proxy developed for SST estimation was the $U^{K'}_{37}$ index [*Prahl and Wakeham*, 1987], based on the relative abundance of di-unsaturated and tri-unsaturated alkenones produced by haptophyte algae [*Brassell et al*., 1986]. Culture and core top studies have shown that this index correlates well with mean annual SST [*Müller et al*., 1998]. However, it has also been shown that physiological growth factors including nutrient and light limitation can affect the $U^{K'}_{37}$ index [*Herbert*, 2003, and references cited therein]. Furthermore, diagenesis may affect $U^{K'}_{37}$ [*Hoefs et al*., 1998; *Gong and Hollander*, 1999]. A more recently developed SST proxy, the TEX^{H}_{86} index, is based on the relative abundance of glycerol dialkyl glycerol tetraethers (GDGTs) [*Schouten et al*., 2002; *Kim et al*., 2010] produced by Thaumarchaeota [*Sinninghe Damsté et al*., 2002]. This proxy has the advantage, compared to the $U^{K'}_{37}$, that it can be applied at temperatures $>28°C$ and in sediments up to 145 Ma old where alkenones are rarely found. Furthermore, it seems to be less affected by diagenesis [*Schouten et al*., 2004; *Kim et al*., 2009]. However, contributions of GDGTs from land can substantially affect the TEX^{H}_{86} [*Weijers et al*., 2006], and additionally, as Thaumarchaeota occur throughout the water column [*Karner et al*., 2001; *Herndl et al*., 2005], TEX^{H}_{86} has been reported to sometimes reflect subsurface temperatures (i.e., below the wind mixed layer) instead of SST [*Huguet et al*., 2007; *Lee et al*., 2008; *Lopes dos Santos et al*., 2010; *Rommerskirchen et al*., 2011; *Kim et al*., 2012]. The newest organic proxy for SST, the LDI (long-chain diol index), has been recently described by *Rampen et al*. [2012] and is based on the relative distribution of long-chain 1,13-diol and 1,15-diol produced by algae, likely eustigmatophytes [*Volkman et al*., 1992]. The LDI shows a strong correlation with mean annual SST in marine surface sediments. Application on a sediment core from the southeastern Atlantic showed SST patterns for the last 43 ka in agreement with other SST proxies and known climate events [*Rampen et al*., 2012]. However, factors other than temperature, which can affect this proxy, have not yet been investigated in any detail. Finally, although all organic proxies are calibrated against annual mean SST using surface sediments, they have sometimes been reported to be biased toward a certain season at certain locations [e.g., *Ternois et al*., 1997; *Sikes et al*., 2002; *Herfort et al*., 2006; *Castañeda et al*., 2010; *Prahl et al*., 2010; *Huguet et al*., 2011]. The application of multiple proxies can potentially yield more insight in these seasonal biases as well as other factors affecting SST reconstructions.

[4] The Southern Ocean has been a target of a large number of paleotemperature studies using the $U^{K'}_{37}$ index and foraminifera-based proxies, especially around New Zealand and Tasmania [e.g., *Ikehara et al*., 1997; *Sikes et al*., 2002; *Pelejero et al*., 2003; *Sikes et al*., 2005; *Nürnberg and Groeneveld*, 2006; *Pahnke and Sachs*, 2006; *Pelejero et al*., 2006; *Barrows et al*., 2007a, 2007b; *Sikes et al*., 2009]. In general, these studies reported that the last interglacial was 1–2°C warmer than the present interglacial [*Ikehara et al*., 1997; *Sikes et al*., 2002; *Nürnberg and Groeneveld*, 2006; *Pahnke and Sachs*, 2006; *Pelejero et al*., 2006; *Barrows et al*., 2007a], and reconstructions of the subtropical front movement on the South Tasman Rise showed that the front was in its farthest north position (around East Tasman Plateau) during the Last Glacial Maximum (LGM) and south of the East Tasman Plateau from 11 to 6 ka [*Sikes et al*., 2009]. In comparison to New Zealand, offshore southeastern Australia has also been the subject of several paleoceanographic studies [*Gingele et al*., 2004; *Gingele and De Deckker*, 2005; *Calvo et al*., 2007; *Gingele et al*., 2007; *Moros et al*., 2009; *Lopes dos Santos et al*., 2012; *De Deckker et al*., 2012], but only a few reconstructions of SST exist [*Wells and Okada*, 1996; *Calvo et al*., 2007].

[5] In this study, we applied multiple SST proxies to a sediment record from the Murray Canyons Group area offshore southeastern Australia (Figure 1). Presently, this area is under the influence of the Leeuwin Current (LC), which is Australia's longest warm water current, and its extensions, the South Australian and Zeehan Currents [*Ridgway and Condie*, 2004] (Figure 1). *Ridgway and Condie* [2004] showed that under modern day conditions, the LC (or its extensions) first penetrates the southern shelf of Australia and reaches the core area in May with the strongest influence in austral winter, i.e., July, especially during La Niña phases. Several paleoceanographic studies have reconstructed the strength and impact of the LC on millennial time scales [*Wells and Wells*, 1994; *Li et al*., 1996; *Li and McGowran*, 1998; *Martinez et al*., 1999; *Li et al*., 1999; *Gingele et al*., 2001; *Barrows and Juggins*, 2005; *Moros et al*., 2009; *Spooner et al*., 2011], but most of these studies focused on the western coast of Australia and it is not clear whether the LC reached South Australian coastal waters during glacial periods. *Wells and Wells* [1994] suggested that the LC was absent during glacials due to an intensification of the West Australian Current and due to higher addition of the Indonesian

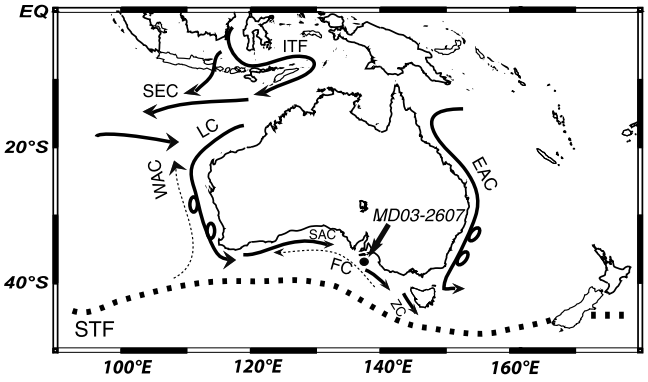

Figure 1. Location of core MD03-2607 offshore southeastern Australia (black dot) together with the modern position of the Subtropical Front (STF; dashed line) and the main currents around Australia (arrows). ITF = Indonesian Throughflow, LC = Leeuwin Current, SAC = South Australia Current, FC = Flinders Current (dotted arrow means subsurface current), ZC = Zeehan Current, WAC = West Australia Current (dotted arrow means subsurface current), EAC = East Australia Current, SEC = South Equatorial Current. The figure is modified from *Lopes dos Santos et al*. [2012]. Map was generated with the Ocean Data View software.

Throughflow waters into the South Equatorial Current instead of the LC. However, *Barrows and Juggins* [2005] and *Spooner et al*. [2011] showed that the LC did not cease, but its temperature decreased during glacials and probably reached latitudes as far as 32°S (see Figure 1). Most studies have found this current to be much more intense during interglacials than during glacials and to reach southeastern Australia or even the west coast of Tasmania [*Wells and Wells*, 1994; *Ridgway and Condie*, 2004; *Moros et al*., 2009; *De Deckker et al*., 2012].

[6] A multiproxy approach is used in this paper to reconstruct SST offshore southeastern Australia for the last ~135 ka. For the first time, we determined SST applying three independent organic proxies (LDI, $U^{K'}_{37}$, and TEX^{H}_{86}) from a single core. We compare these organic proxy records with foraminiferal assemblages also from the same sediment core, which allows us to assess potentially biases and seasonal contrasts of these proxy records and possibly to assess the impact of the LC as it mainly affects this site during winter. The results provide an improved understanding of the application of these SST proxies in this region of the Southern Ocean and a good comparison with previous studies from east of Tasmania and around New Zealand.

2. Materials and Methods

[7] Sediment core MD03-2607 was recovered during the AUSCAN 2003 cruise (MD131) from the Murray Canyons Group area offshore southeastern Australia at 36°57.64′S and 137°24.39′E (Figure 1) in 865 m water depth [*Hill and De Deckker*, 2004]. A description of the core and its mineralogical content can be found in *Gingele et al*. [2004]. The age model of this core was recently revised by *Lopes dos Santos et al*. [2012] and is based on 22 ^{14}C dates of mixed planktonic foraminiferal assemblages (*Globigerina bulloides* and *Globigerinoides ruber*) and 13 optically stimulated luminescence dates of single grains or small aliquots of sand-sized quartz for the past ~35 ka (first 430 cm of the core) following the methods described in *Wilkins* [2009]. The age model of the lower part of the core is based on correlation of the $\delta^{18}O$ record of the planktonic foraminifera *Globigerina bulloides* with the stacked isotope record of *Lisiecki and Raymo* [2005].

2.1. Sampling of Core MD03-2607

[8] Initial onboard analysis, during the 2003 AUSCAN cruise, indicated higher sedimentation rates toward the base of the core MD03-2607 (~30 m long), and this was considered during sampling. For biogeochemical analyses, only the first 15 m of the core was sampled with a resolution of 5 cm intervals for the first 3 m and at 10 cm for the rest 12 m. A total of 172 samples were analyzed. For the relative foraminiferal abundance counts, the entire core was sampled; however, for this study, only data of the first 15 m are reported. The Holocene section was sampled every 5 cm, but sections with higher sedimentation rates were increased to a sampling rate of 20, 30, and 60 cm. Foraminifera counts were made for a total of 116 samples.

2.2. Biomarker Analysis

[9] Sediment samples were freeze-dried, homogenized, and extracted using an automated solvent extractor (ASE 200, Dionex), 100°C, and 7.6×10^6 Pa with a mixture of dichloromethane (DCM):methanol (MeOH) (9:1, *v*:*v*) to obtain a total lipid extract (TLE). Internal standards (squalane, nonadeca-1-one, C_{46} GDGT) were added to the TLE, which was subsequently separated into an apolar, ketone, and polar fraction in an alumina oxide column (Al_2O_3), using *n*-hexane/DCM 9:1, *n*-hexane/DCM 1:1, and methanol/DCM 1:1 as eluents, respectively. The ketone fractions, containing the alkenones, were analyzed by gas chromatography (GC) and gas chromatography/mass spectrometry (GC/MS) as described previously [*Lopes dos Santos et al*., 2012]. One aliquot of the polar fraction was analyzed for GDGTs by filtration through a polytetrafluoroethylene filter and analyzed using high-performance liquid chromatography/mass spectrometry (HPLC/MS) following *Schouten et al*. [2007]. Another aliquot of the polar fraction was analyzed for long-chain diols by sylilation using bis(trimethylsilyl)trifluoroacetamide and pyridine before being analyzed by GC/MS following *Rampen et al*. [2012]. The analytical error for all the proxies, based on duplicate analysis, was <0.5°C.

2.2.1. $U^{K'}_{37}$ Analyses

[10] Alkenone identification and analysis have been described in *Lopes dos Santos et al*. [2012]. Briefly, the ketone fraction was analyzed by a Hewlett Packard 6890 GC, fitted with a 50 m fused silica column with 0.32 mm diameter and coated with CP Sil-5 (thickness = 0.12 μm). The carrier gas was helium. The oven was programmed from 70°C at injection, then increased by 20°C min^{-1} to 200°C and next by 3°C min^{-1} until 320°C. The final temperature of 320°C was held for 30 min. The $U^{K'}_{37}$ was calculated using the equation described by *Prahl and Wakeham* [1987]. SST values were estimated using the global core top calibration of *Müller et al*. [1998] covering a temperature range of 0 to 27°C and having a calibration error of 1.5°C.

2.2.2. LDI Analyses

[11] Compound identification of the long-chain diols was conducted using a Thermofinnigan Trace GC Ultra connected

to Thermofinnigan DSQ MS operated at 70 eV, with a mass range of *m/z* 50–800 and three scans per second. The capillary column was a silica column (25 m × 0.32 mm) coated with CP Sil-5 (film thickness = 0.12 μm). The initial oven temperature started at 70°C and increased at a rate of 20°C min^{-1} to 130°C and subsequently at a rate of 4°C min^{-1} to the final temperature of 320°C, which was held for 10 min. The relative abundance of diols was measured using single ion monitoring of *m/z* 299, 313, 327, and 411 with a dwell time of 100 ms. The LDI index was calculated using equation (1), as described by *Rampen et al*. [2012]:

$$\mathrm{LDI} = \frac{[\mathrm{C_{30}}1,15\text{-diol}]}{[\mathrm{C_{30}}1,15\text{-diol}] + [\mathrm{C_{28}}1,13\text{-diol}] + [\mathrm{C_{30}}1,13\text{-diol}]}. \quad (1)$$

[12] It was converted into SST using the global core top calibration of *Rampen et al*. [2012], covering a temperature range of −3 to 27°C, and reported to have a calibration error of 2°C:

$$\mathrm{SST} = \frac{\mathrm{LDI} - 0.095}{0.033}. \quad (2)$$

2.2.3. TEX^{H}_{86} Analyses

[13] The polar fractions were analyzed for GDGTs using HPLC-atmospheric pressure chemical ionization (APCI)-MS following *Schouten et al*. [2007]. TEX^{H}_{86} was calculated using equation (3) described by *Kim et al*. [2010], and equation (4) was used to estimate temperature values. This global core top calibration, covering a temperature range of −3 to 30°C, was reported to comprise a calibration error of 2.5°C [*Kim et al*., 2010]:

$$\mathrm{TEX}^{\mathrm{H}}_{86} = \log\left(\frac{[\text{GDGT-2}] + [\text{GDGT-3}] + [\text{Cren}']}{[\text{GDGT-1}] + [\text{GDGT-2}] + [\text{GDGT-3}] + [\text{Cren}']}\right), \quad (3)$$

where GDGT-*x* refers to the GDGT with *x* number of cyclopentane moieties and "Cren′" refers to the crenarchaeol regio-isomer.

$$\mathrm{SST} = 68.4\left(\mathrm{TEX}^{\mathrm{H}}_{86}\right) + 38.6 \quad (4)$$

2.2.4. BIT Analyses

[14] The branched GDGTs, derived from soil bacteria, and crenarchaeol were analyzed using HPLC-APCI-MS following *Hopmans et al*. [2004]. The branched isoprenoid tetraether (BIT) index, a proxy for soil organic matter input into the marine environment, was calculated using equation (5) described by *Hopmans et al*. [2004]:

$$\text{BIT index} = \frac{[\text{br GDGT I}] + [\text{br GDGT II}] + [\text{br GDGT III}]}{[\text{br GDGT I}] + [\text{br GDGT II}] + [\text{br GDGT III}] + [\text{Cren}]}. \quad (5)$$

2.3. Planktonic Foraminifera Analyses and Modern Analogue Technique

[15] The species nomenclature used in this study follows the taxonomy of *Saito et al*. [1981]. Counts of planktonic foraminifera were made on splits of the >150 μm fraction removing small juvenile specimens. Each sample was split by an Otto microsplitter until ~400 species were present in the final split.

[16] SST was estimated from the planktonic foraminiferal assemblage data using the modern analogue technique, in conjunction with a database from Southern Hemisphere core tops, AUSMAT-F4, with a final training set containing 1303 core top samples [*Barrows and Juggins*, 2005]. The annual SST (T_{mean}) and the temperature of the warmest (T_{max}) and coolest months (T_{min}) were estimated, with each estimate calculated as the mean of the 10 best analogues from the global database. The distance to the nearest analogue, the mean distance, and the standard deviation were also calculated to assess the quality of the analogue. The relatively most precise variable, for the temperature range of −1 to 30°C, is T_{mean} with a root mean squared error of prediction (RMSEP) of 0.8°C based on a fivefold leave-out cross validation (note that this is a different method for error calculation than those for the organic proxies which is based on global calibration errors). T_{max} also has a low RMSEP of 0.9°C, whereas T_{min} SST has relatively the greatest error with a RMSEP of 1°C [*Barrows and Juggins*, 2005]. The quality of SST estimates is measured by the squared chord distance, with distances of <0.2 indicating good analogues (for further details, see *Barrows and Juggins* [2005]).

3. Results

[17] As previously discussed in *Lopes dos Santos et al*. [2012], the $U^{K'}_{37}$ SST estimates follow the same trend as the $\delta^{18}O$ record of the planktonic foraminifera *Globigerina bulloides* (Figures 2a and 2b). The highest SST inferred by the $U^{K'}_{37}$ is ~21°C during the last interglacial (123 ka), slightly higher than the $U^{K'}_{37}$ SST estimate of the present interglacial of 20°C at 4.5 ka. $U^{K'}_{37}$ SST increases by 10°C during the transition from the LGM to the Holocene [*Lopes dos Santos et al*., 2012] with an interruption from ~16 to 13 ka in the warming trend. The TEX^{H}_{86} (blue line, Figure 2b) shows the highest SST of ~21°C during the last interglacial at 127 ka and the lowest SST of ca. 8°C during the LGM and marine isotope stage (MIS) 4. Similar to the $U^{K'}_{37}$, the TEX^{H}_{86} temperature estimates rise by up to 10°C during the last deglaciation with an interruption from ~16 to 13 ka. The TEX^{H}_{86} follows the same trend as the $U^{K'}_{37}$ (red line, Figure 2b) and $\delta^{18}O$ (Figure 2a; from *Lopes dos Santos et al*. [2012]) records, but absolute SSTs are generally lower than $U^{K'}_{37}$ by up to 6°C, except during deglaciation and interglacials (MIS 1 and 5e) where they are similar to $U^{K'}_{37}$ temperatures. The LDI-derived SST (green line, Figure 2b) has the highest value of ~25°C during MIS 5e around 121 ka, which is slightly higher than the late Holocene LDI temperature of ~24°C. The lowest LDI temperature of ~13°C was recorded during the LGM. The LDI also shows a warming of 11°C during deglaciation and an interruption of the deglacial warming trend from ~16 to 13 ka. The LDI record has a similar trend as the other SST records, but absolute values are consistently higher than those of $U^{K'}_{37}$ and TEX^{H}_{86} temperatures by up to 9°C, except during deglacial periods when temperature estimates are similar to those of $U^{K'}_{37}$ and TEX^{H}_{86}.

[18] The foraminiferal assemblage temperature estimates all show the same trend as the organic proxies with highest SST during the last interglacial and lowest SST during glacial periods (Figures 2b and 2c). However, from ~16 to 13 ka,

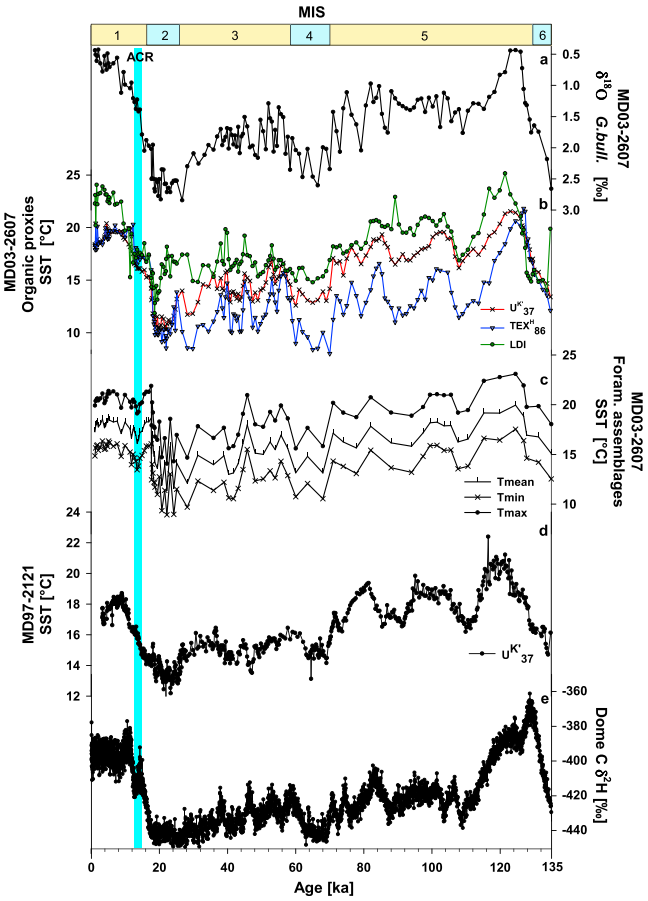

Figure 2. Planktonic foraminiferal oxygen isotopes and SST reconstructions from core MD03-2607 and core MD97-2121, together with the Dome C deuterium isotope record, as a proxy for air temperature in Antarctica. All proxies show temperature changes coherent with each other as well as those of other locations, suggesting they track Southern Hemisphere climate change. (a) $\delta^{18}O$ record of *Globigerina bulloides* [*Lopes dos Santos et al*., 2012]; (b) LDI SST in green, TEX^{H}_{86} SST in blue, and $U^{K'}_{37}$ SST in red ($U^{K'}_{37}$ SST from *Lopes dos Santos et al*., 2012]; (c) modern analogue technique SST reconstructions for warm months (dots), cold months (crosses), and mean annual (vertical lines); (d) $U^{K'}_{37}$ SST reconstructions from subtropical waters at site MD97-2121, east of New Zealand using the *Müller et al*. [1998] calibration [*Pahnke and Sachs*, 2006]; (e) $\delta^{2}H$ from the EPICA ice core, Dome C [*Jouzel et al*., 2007]. The shaded bar is the Antarctic Cold Reversal (ACR). MIS = marine isotope stage.

a sharp cooling is observed instead of an interruption as recorded by the organic proxies, and the magnitude of temperature change during the last deglaciation is ~8°C. The foraminiferal assemblages provide a mean annual SST estimate of ~20°C during the last interglacial period, which is slightly higher than the present interglacial SST of ~19°C (Figure 2c), and the lowest mean annual SST (T_{mean}) of ~11°C was recorded during the LGM. The SST of the warmest month (T_{max}) is estimated at ~22–23°C during the interglacials and at ~14°C during the LGM (Figure 2c). The coldest month SST (T_{min}) was ~18°C during interglacials and ~9°C during LGM (Figure 2c).

4. Discussion

4.1. Comparison of SST Estimates

[19] The organic and faunal proxy SST records (Figures 2a–2c) all broadly follow the trend of the $\delta^{18}O$ record of *G. bulloides*, and all are generally in line with previously obtained SST records of subtropical waters of the Southern Ocean east of New Zealand [e.g., *Pahnke and Sachs*, 2006] (Figure 2d) and with changes in Antarctic temperature reconstructed from the $\delta^{2}H$ record of the European Project for Ice Coring in Antarctica (EPICA) Dome C ice core (Figure 2e) [*Jouzel et al*., 2007]. This collectively suggests that the SST in the Murray Canyons Group area follows Southern Hemisphere climate variations as previously suggested for the last 30 ka [*Calvo et al*., 2007]. The coherent changes between the organic proxy SST records are evident from the significant correlation between them ($r^2 = 0.62$–0.66, $p < 0.001$), with only TEX^{H}_{86} and LDI showing a weaker but still significant ($r^2 = 0.37$, $p < 0.001$) correlation (Figure 3). Importantly, the timing and trends of the SST changes do not differ substantially between the organic proxies and the foraminiferal temperature records, suggesting that the former are not strongly affected by lateral transport or selective degradation. A similar observation was made for subtropical waters from east of New Zealand, where SST estimates based on $U^{K'}_{37}$ were comparable to those based on foraminiferal assemblages (using modern analogue technique) for the last 60 ka [*Sikes et al*., 2002].

[20] The magnitude of temperature variations and absolute temperature values between the three organic proxies are different in the Murray Canyons Group area. For some part, this difference between the SST estimates is within calibration errors of the proxies. The calibration errors were reported to be 1.5°C for $U^{K'}_{37}$ [*Müller et al*., 1998], 2.5°C for TEX^{H}_{86} [*Kim et al*., 2010], and 2.0°C for LDI [*Rampen et al*., 2012], which may result in offsets of up to 3.5°C between different proxy records. However, for large parts of the record, differences in SST reconstructed using these three proxies are >3.5°C. Apparently, this needs to be explained by factors other than calibration errors. Furthermore, these observed offsets are variable and not systematic in nature and thus cannot be explained by calibration issues only. Each proxy can be affected by a variety of parameters other than temperature. For instance, soil organic matter input by rivers may affect GDGT distributions in coastal marine sediments and thus TEX^{H}_{86} [*Weijers et al*., 2006]. However, the BIT index, a proxy for soil organic matter input in the marine environment [*Hopmans et al*., 2004], was always <0.3, suggesting that TEX^{H}_{86} was not substantially affected by soil organic matter input [cf. *Weijers et al*., 2006]. The LDI and $U^{K'}_{37}$ are not expected to be influenced by soil organic matter input because they are likely to be uniquely sourced by algae. Lateral transport and selective degradation are unlikely to be an important issue as discussed above. Light and nutrient limitation may affect some of the organic proxies [e.g., *Epstein et al*., 1998; *Prahl et al*., 2005; *Sikes et al*., 2005]. For instance, *Sikes et al*. [2005] already postulated that alkenone temperatures obtained from two sediment traps offshore New Zealand were relatively low compared to SST as a result of nutrient limitation effects. However, it is not clear how these

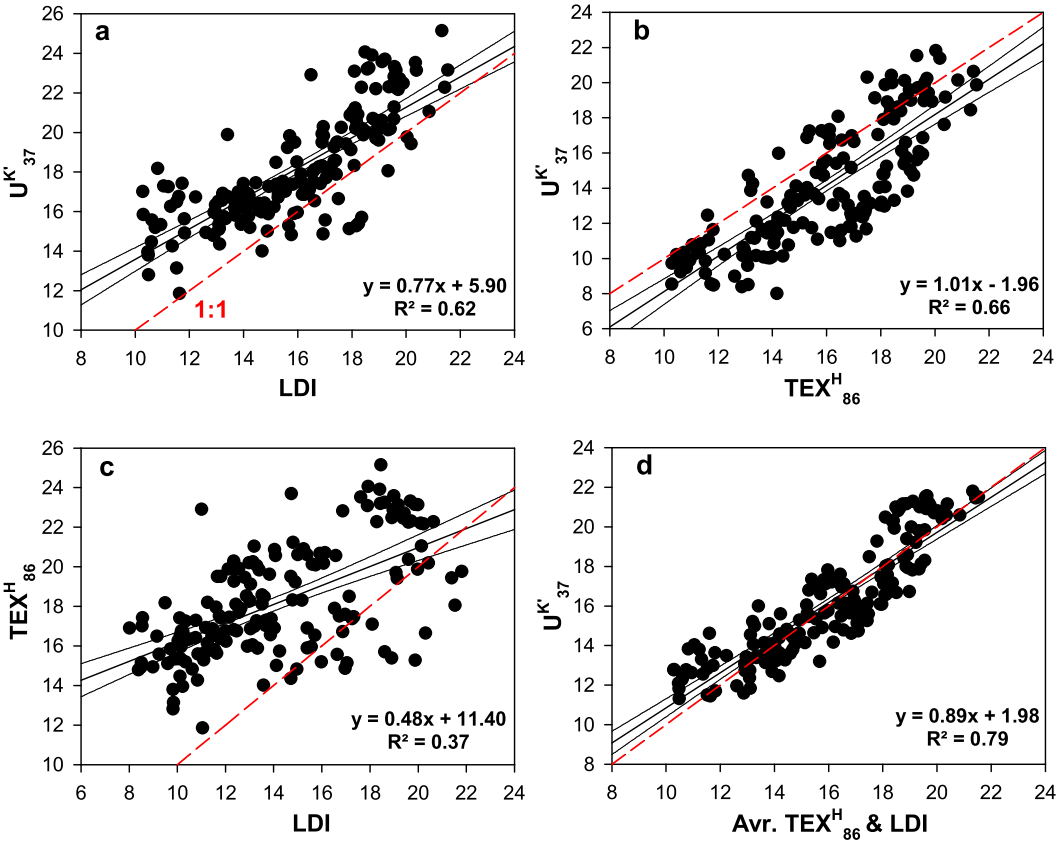

Figure 3. Correlations and confidence intervals (95%) between organic proxy SST estimates for core MD03-2607. Correlation (a) between $U^{K'}_{37}$ and LDI, (b) between $U^{K'}_{37}$ and TEX^{H}_{86}, (c) between TEX^{H}_{86} and LDI, and (d) between $U^{K'}_{37}$ and the average of the TEX^{H}_{86} and LDI. The red dashed line is the 1:1 line. All correlations are significant, i.e., p values are <0.001.

factors would affect the proxies such that they would cause the observed differences in SST.

[21] The proxies most likely record the growth temperature of their source organisms, and therefore, the different SST estimates might be influenced by the difference in the depth habitat of the organisms. Thaumarchaeota are chemoautotrophic nitrifiers [*Könneke et al.*, 2005; *Wuchter et al.*, 2006; *Park et al.*, 2010] and occur throughout the water column [e.g., *Karner et al.*, 2001; *Herndl et al.*, 2005], and therefore, the TEX^{H}_{86} may record lower temperatures of deeper water masses than the LDI and $U^{K'}_{37}$ proxies, as proposed previously [e.g., *Lee et al.*, 2008; *Lopes dos Santos et al.*, 2010; *Kim et al.*, 2012]. However, TEX^{H}_{86} temperatures are not always lower than the $U^{K'}_{37}$; for example, during the deglaciations, TEX^{H}_{86} temperatures are similar to those of the LDI and $U^{K'}_{37}$. This may suggest that Thaumarchaeota did migrate between the surface and the subsurface in the water column during specific periods. For the LDI and $U^{K'}_{37}$ proxies, the same reconstructed temperatures would be expected because both proxies are based on biomarkers produced by photosynthetic algae. However, the LDI is recording higher temperatures than $U^{K'}_{37}$, a feature which is difficult to explain by differences in depth habitat.

[22] Thus, most factors known to affect the different proxies are unlikely to explain the differences observed between their SST estimates. One last explanation for the dissimilarity between the reconstructed SST estimates may be differences in the growing season of the source organisms of each of the biomarkers. Unfortunately, no information on the seasonality effect on TEX^{H}_{86} and LDI is yet available for the Southern Hemisphere.

4.2. Seasonal Influences on the Organic Proxy Records

[23] To examine the impact of seasonality on the organic proxies, we compared SST estimates from the uppermost core sample with SSTs of the present day system in different seasons (Figure 4). The LDI gives a temperature estimate of 22°C, which is 4°C higher than the SST recorded during austral summer at our core site [*Locarnini et al.*, 2010]. TEX^{H}_{86} and $U^{K'}_{37}$ estimate a temperature of 18°C that matches modern austral summer SST but is 2°C higher than annual mean SST. Interestingly, the SST estimates based on the foraminiferal assemblage are also generally higher than modern SST but close to the estimated uncertainties (Figure 4), with the T_{max} and T_{min} ~1°C higher than the modern warmest and coolest temperature, respectively, while T_{mean} is also ~1°C higher than modern SST (Figure 4). Our age model suggests that the uppermost sample is ~1 ka old. So it is therefore possible that these reconstructed high temperatures indicate that the uppermost sediment of our core does not represent modern conditions and thus may be from a warmer period in the past. Indeed, the $U^{K'}_{37}$ SST estimate at ~1 ka from the nearby core MD03-2611 (36°44′S, 136°33′E [*Calvo et al.*, 2007]) is 0.5°C warmer than the uppermost sediment dating 0.7 ka.

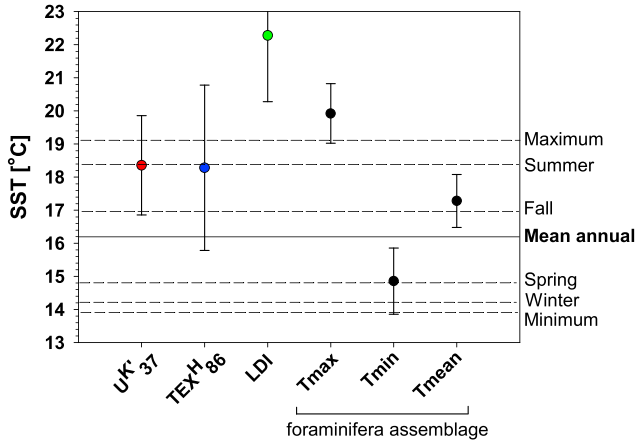

Figure 4. Measured and proxy reconstructed SST (from the core top) at core site MD03-2607. Modern austral seasonal SST, mean annual SST, and minimum and maximum SST [*Locarnini et al.*, 2010] are shown as lines together with reconstructed SST based on organic proxies (colored dots) and based on foraminifera assemblages (black dots). Error bars represent calibration errors of the proxies, i.e., 1.5°C for $U^{K'}_{37}$ [*Müller et al.*, 1998], 2.5°C for TEX^{H}_{86} [*Kim et al.*, 2010], 2.0°C for LDI [*Rampen et al.*, 2012], and 0.8–1°C for the foraminifera assemblages [*Barrows and Juggins*, 2005]. Within these calibration errors, $U^{K'}_{37}$ and TEX^{H}_{86} temperatures are close to the fall/mean modern SST, and LDI is close to warmest modern SST. The foraminifera assemblage warmest month, mean annual, and coldest month temperatures are close to the maximum, mean, and minimum SST, respectively.

Furthermore, the uppermost sediment sample from core V18-222 in southeastern Australia (38°34′S, 140°37′E [*Wells and Okada*, 1996]) dated at ~2 ka showed a summer SST temperature estimate ~1°C warmer than the present day [*Locarnini et al.*, 2010]. Therefore, and taking into account the calibration errors discussed above, the LDI may represent austral summer temperatures, TEX^{H}_{86} and $U^{K'}_{37}$ represent annual mean or austral fall temperatures, while the SST estimates from foraminiferal assemblages would fit the seasonal SST distribution at the Murray Canyon area (Figure 4).

[24] To test the potential impact of seasonality on the organic proxies over a geological time scale, we compared the organic proxy-derived SST records with seasonal SSTs obtained from the foraminiferal assemblages (Figure 5). A previous sediment trap study east of New Zealand showed that the latter proxy represented seasonal SST well [*King and Howard*, 2001]. Additionally, SST estimates derived from foraminiferal assemblages [*Barrows et al.*, 2007a] reflected different absolute temperatures than the mean annual SST estimated by $U^{K'}_{37}$ [*Pelejero et al.*, 2006] in the Tasman Sea. Contrary to this, $U^{K'}_{37}$ sediment trap and down core studies performed east of New Zealand and from the Tasman Plateau showed that $U^{K'}_{37}$ temperature estimates correlated well with summer SST [*Sikes et al.*, 2002, 2005; *Pahnke and Sachs*, 2006]. Therefore, a comparison between the organic and inorganic proxies may clarify the impact of seasonality on these proxies at our study site.

[25] The comparison between the organic and inorganic proxies shows that the LDI-reconstructed SSTs follow a similar trend and have similar absolute values as the warmest month SSTs (T_{max}) reconstructed from foraminiferal assemblages

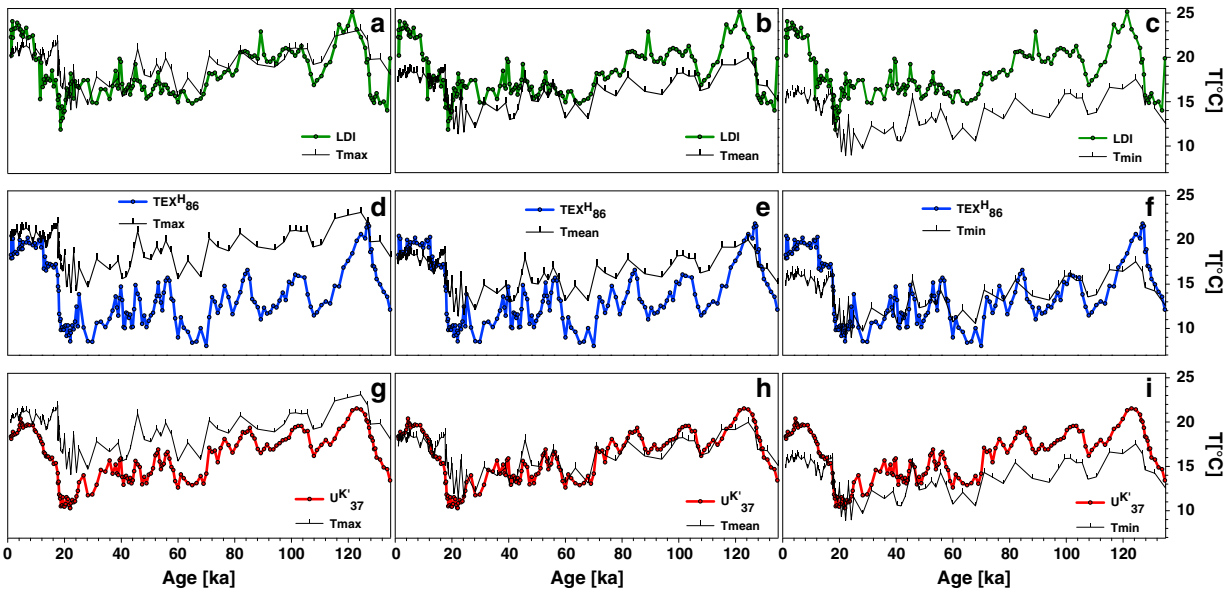

Figure 5. Comparison of paleotemperatures reconstructed with organic proxies with those reconstructed with the modern analogue technique of foraminifera assemblages from core MD03-2607. The figure shows LDI SST together with foraminifera SST reconstruction for the (a) warmest months (T_{max}), (b) annual (T_{mean}), and (c) coldest months (T_{min}); (d–f) TEX^{H}_{86} SST together with foraminifera SST reconstruction in the same order as described for LDI; and (g–i) $U^{K'}_{37}$ SST (from *Lopes dos Santos et al.* [2012]) with SST reconstruction using assemblages in the same order described above. The comparisons show that $U^{K'}_{37}$, TEX^{H}_{86}, and LDI most closely match mean annual, minimum, and maximum faunal-based temperatures, respectively.

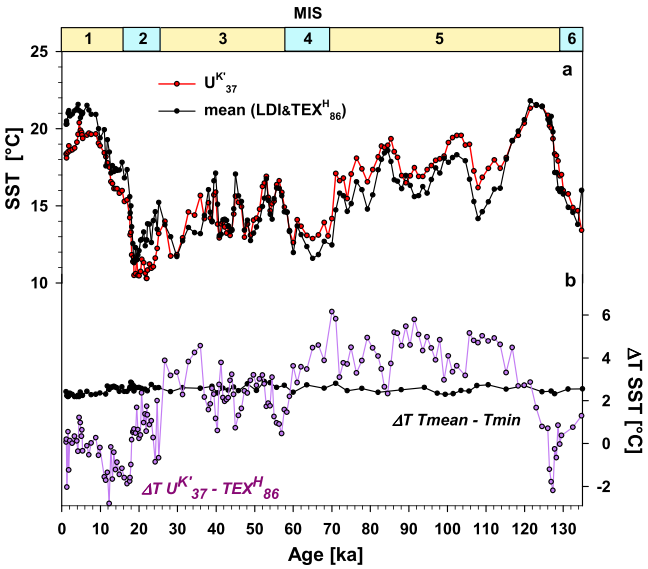

Figure 6. Reconstructed SST and seasonality changes from southeastern Australia (core MD03-2607). (a) Comparison of the $U^{K'}_{37}$ SST record [*Lopes dos Santos et al.*, 2012] with the mean of the LDI and TEX^{H}_{86} SST estimates, demonstrating a good match between these estimates. (b) Differences between reconstructed seasonality based on the difference between the mean annual and coolest months from the foraminiferal assemblages (black line) and the difference between $U^{K'}_{37}$ and TEX^{H}_{86} (purple line).

throughout most of the core (Figure 5a–5c). In contrast, TEX^{H}_{86}-reconstructed SSTs are more in agreement with the coolest month SSTs (T_{min}), except during interglacials where TEX^{H}_{86} SST estimates are 4–5°C warmer than T_{min} (Figures 5d–5f). Finally, $U^{K'}_{37}$-reconstructed SSTs are in good agreement with the mean annual SSTs (T_{mean}) reconstructed using the foraminiferal assemblages (Figures 5g–5i). Together, this strongly suggests that LDI and TEX^{H}_{86} proxies may reflect SST of a particular season, i.e., warm austral summer and cold austral winter, respectively, while $U^{K'}_{37}$ records the mean annual SST. Further support for this interpretation comes from the fact that the average of SST estimates using LDI and TEX^{H}_{86} yields a composite SST record that correlates well with the $U^{K'}_{37}$ record (Figures 6a and 3d).

[26] Previous studies have shown that TEX^{H}_{86} can record seasonal rather than annual mean SST. For example, *Herfort et al*. [2006] showed that the TEX_{86} recorded mainly winter temperatures in the southern North Sea, whereas for the Mediterranean, it was shown that TEX^{H}_{86} likely recorded summer temperatures [*Menzel et al*., 2006; *Leider et al*., 2010; *Castañeda et al*., 2010; *Huguet et al*., 2011]. The seasonal bias toward winter temperatures in the North Sea [*Herfort et al*., 2006] was attributed to the higher abundance of Thaumarchaeota during this season in this area [*Wuchter et al*., 2006; *Pitcher et al*., 2011]. During winter, the concentration of ammonia, which fuels the chemoautotrophic Thaumarchaeota, is high and algal productivity is low, and thus, competition for ammonia is limited. At our site, it is possible that the growth season of Thaumarchaeota is also related to higher ammonia levels and less competition with algae in austral winter. Indeed, chlorophyll abundances are on average generally low during austral winter compared to austral fall and spring [*Conkright et al*., 2002]. However, for a better understanding of the influence of seasonality in the TEX^{H}_{86} proxy, ecological studies of Thaumarchaeota as well as sediment trap studies are needed.

[27] For $U^{K'}_{37}$, a seasonal bias has sometimes been observed [*Ternois et al*., 1997; *Sikes et al*., 2005; *Castañeda et al*., 2010; *Leider et al*., 2010; *Prahl et al*., 2010]. Specifically for the Southern Ocean, $U^{K'}_{37}$ SST correlated well with summer SST [*Ikehara et al*., 1997; *Sikes et al*., 2002, 2005; *Pahnke and Sachs*, 2006]. Sediment trap studies from the east of New Zealand showed that fluxes of alkenones mainly peaked in spring-summer [*Nodder and Northcote*, 2001; *Sikes et al*., 2005], and that may possibly explain the better correlation of $U^{K'}_{37}$ temperature estimates with summer temperatures. However, this proxy generally shows a stronger relationship with the mean annual SST in other regions of the Southern Ocean [*Pelejero et al*., 2006; *Calvo et al*., 2007] and in many other oceanic areas [e.g., *Müller et al*., 1998; *Herbert*, 2003, and references cited therein; *Mohtadi et al*., 2011], as observed at our location. Possibly, the $U^{K'}_{37}$ proxy is not affected by seasonal growth of the alkenone producers in southeastern Australian waters, or that due to "time averaging effect," this seasonality is not reflected downcore. For LDI, no studies have been done yet on seasonal biases. However, a slightly stronger correlation of LDI values with summer SST compared to an annual mean was reported by *Rampen et al*. [2012] for marine surface sediments, tentatively suggesting that the source organisms, likely eustigmatophyte algae [*Volkman et al*., 1992], may preferentially proliferate during summer months. Our LDI record also suggests that the source algae for the diols may be more abundant during austral summer, although this season's chlorophyll concentrations are relatively low in comparison to the fall season's [*Conkright et al*., 2002]. Sediment trap studies are clearly needed to confirm a seasonality effect for this new proxy. Nevertheless, our results clearly show that the LDI is a promising new proxy to reconstruct SST and can give insights into SST changes complementary to other (organic) SST proxies.

4.3. Convergence of TEX^{H}_{86} and $U^{K'}_{37}$ SST Estimates During Deglaciations

[28] An intriguing observation is that the differences in SST as determined by the organic proxies, in particular the TEX^{H}_{86} and $U^{K'}_{37}$, are much smaller during deglaciations and interglacials. Comparison of our $U^{K'}_{37}$ SST record with that of the nearby core MD03-2611 (~80 km away) [*Calvo et al*., 2007] shows a good match confirming that the $U^{K'}_{37}$ is giving a regionally consistent pattern, whereas TEX^{H}_{86} follows this pattern only during deglaciation and interglacials.

[29] Two explanations can be proposed for this decrease in the difference between the reconstructed temperatures using $U^{K'}_{37}$ and TEX^{H}_{86} at our site. First, it could be that the Thaumarchaeota changed their growth season during deglaciations and interglacials and were more reflective of annual mean temperatures, matching the $U^{K'}_{37}$ temperature estimates. Indeed, a relatively lower temperature difference between TEX^{H}_{86} and $U^{K'}_{37}$ was also recorded during interglacials in the Mediterranean and was explained by a change in growth season for the Thaumarchaeota [*Castañeda et al*., 2010; *Huguet et al*., 2011]. A similar situation where Thaumarchaeota may have been changing their behavior

during interglacials may have occurred here, although ecological and sediment trap studies are required to confirm this hypothesis.

[30] Second, it could be that winter temperatures, as recorded by TEX^{H}_{86} at this site, were relatively warm during deglaciations, causing a decrease in the differences between TEX^{H}_{86} and $U^{K'}_{37}$ SST. However, a warmer austral winter temperature is not apparent in the T_{min} record inferred from the foraminiferal assemblages (Figure 5f), possibly because T_{min} reflects the coldest month, whereas TEX^{H}_{86} may reflect winter temperatures of a different month or the whole winter season. Possibly, TEX^{H}_{86} reflects temperatures from the winter months influenced by warmer water masses (e.g., the LC current), whereas T_{min} does not record this influence. Indeed, seasonality recorded by the difference between T_{mean} and T_{min} inferred by the foraminiferal assemblage is almost constant over the last 135 ka in contrast to the difference between the $U^{K'}_{37}$ and TEX^{H}_{86} proxies (Figure 6b). This suggests that SST reconstructions based on T_{min} and TEX^{H}_{86} are registering different seasonal conditions and are likely to be affected by different factors.

[31] If the relatively high TEX^{H}_{86} SST does indicate a warming of austral winter SST in southeastern Australia, then it is likely reflecting the input of warm waters from the LC (and its extensions) during these periods. If so, this suggests that the LC reached the core site during deglaciations, interglacials, and possibly during MIS 2 and parts of MIS 3 (Figure 2b). Changes in planktonic foraminifera groups also recorded the presence of the LC in the nearby core MD2611 during these periods [*De Deckker et al*., 2012]. The TEX^{H}_{86} SST estimates converge with those of $U^{K'}_{37}$ at ~25 ka, suggesting the presence of the LC from this time period at the core site in the last glacial-interglacial cycle. Because the LC is prevented from reaching southern Australia when the Subtropical Front (STF) was in its northernmost position [*Moros et al*., 2009; *De Deckker et al*., 2012], our results support a southern position of the STF during deglaciations and interglacial, as previously suggested by *Wells and Okada* [1996] and *Barrows et al*. [2000] for the southeastern Australian region, and also during early MIS 2 and parts of MIS 3, as suggested by other studies from the South Tasman Rise [*Sikes et al*., 2009], Indian Ocean [*Bard and Rickaby*, 2009], and southeastern Australia [*De Deckker et al*., 2012]. Indeed, *G. ruber* and *G. sacculifer* were found in the glacial sediments of our core which indicates the presence of subtropical water. Our interpretation is also consistent with the results of *Nürnberg and Groeneveld* [2006] who did not find strong changes in SST and sea surface salinity on the East Tasman Plateau for the last 130 ka, although this was explained by the influence of the East Australian Current which dampened the signal of STF movements. Nevertheless, care has to be taken in reconstructing the LC influence in southeastern Australia and STF position based on the TEX^{H}_{86} due to the uncertainties in interpreting the TEX^{H}_{86} as a winter temperature signal and in interpreting the front as a purely temperature-defined feature.

5. Conclusions

[32] Sea surface temperatures from the Murray Canyons Group area offshore southeastern Australia were reconstructed for the last 135 ka using, for the first time, three independent organic proxies, which showed coherent patterns over glacial-interglacial time scales. Comparison between the SST estimates obtained from organic proxies, modern temperature at the core site, and seasonal SST estimates obtained from foraminiferal assemblages showed that LDI seems to be related to austral summer month SST, TEX^{H}_{86} to austral winter month SST, and $U^{K'}_{37}$ to the mean annual SST. The reduced difference between TEX^{H}_{86} and $U^{K'}_{37}$ SST estimates during the deglaciations is either due to a change in the growth season of Thaumarchaeota or due to a reduced seasonal SST contrast. The difference also possibly shows the impact of the LC during the coolest months at the Murray Canyons Group area because the LC mainly affects winter temperatures offshore southeastern Australia. On a more general level, our study shows that the LDI is a promising new SST proxy which can provide complementary information to that of other commonly used SST proxies. This allowed a unique multiproxy approach, which enabled to evaluate the seasonal biases on the SST proxies. This approach allows a much better understanding of the application of these SST proxies and, consequently, a more robust SST reconstruction from the Southern Ocean region and likely from similar settings elsewhere.

[33] **Acknowledgments.** We thank C. Charles, B.E. Rosenheim, and an anonymous reviewer for their comments which improved the manuscript. Research funding was provided by a VICI grant to SS from the Netherlands Organization of Scientific Research. Core MD03-2607 was obtained with a National Oceans Office and Australian Research Council grant, both awarded to P.D.D. Y. Balut from IPEV was instrumental in obtaining the core. M.I.S. was the recipient of an ANU postgraduate award.

References

Andreasen, D. J., and A. C. Ravelo (1997), Tropical Pacific Ocean thermocline depth reconstructions for the last glacial maximum, *Paleoceanography*, *12*, 395–413.

Bard, E., and R. E. M. Rickaby (2009), Migration of the subtropical front as a modulator of glacial climate, *Nature*, *460*, 380–U93.

Barrows, T. T., and S. Juggins (2005), Sea-surface temperatures around the Australian margin and Indian Ocean during the Last Glacial Maximum, *Quat. Sci. Rev.*, *24*, 1017–1047.

Barrows, T. T., S. Juggins, P. De Deckker, J. Thiede, and J. I. Martinez (2000), Sea-surface temperatures of the southwest Pacific Ocean during the Last Glacial Maximum, *Paleoceanography*, *15*, 95–109.

Barrows, T. T., S. Juggins, P. De Deckker, E. Calvo, and C. Pelejero (2007a), Long-term sea surface temperature and climate change in the Australian–New Zealand region, *Paleoceanography*, *22*, PA2215, doi:10.1029/2006PA001328.

Barrows, T. T., S. J. Lehman, L. K. Fifield, and P. De Deckker (2007b), Absence of cooling in New Zealand and the adjacent ocean during the Younger Dryas chronozone, *Science*, *318*, 86–89.

Brassell, S. C., G. Eglinton, I. T. Marlowe, U. Pflaumann, and M. Sarnthein (1986), Molecular stratigraphy: A new tool for climatic assessment, *Nature*, *320*, 129–133.

Brown, S. J., and H. Elderfield (1996), Variations in Mg/Ca and Sr/Ca ratios of planktonic foraminifera caused by postdepositional dissolution: Evidence of shallow Mg-dependent dissolution, *Paleoceanography*, *11*, 543–551.

Calvo, E., C. Pelejero, P. De Deckker, and G. A. Logan (2007), Antarctic deglacial pattern in a 30 kyr record of sea surface temperature offshore South Australia, *Geophys. Res. Lett.*, *34*, L13707, doi:10.1029/2007GL029937.

Castañeda, I. S., E. Schefuß, J. Pätzold, J. S. Sinninghe Damsté, S. Weldeab, and S. Schouten (2010), Millennial-scale sea surface temperature changes in the eastern Mediterranean (Nile River Delta region) over the last 27,000 years, *Paleoceanography*, *25*, PA1208, doi:10.1029/2009PA001740.

Conkright, M. E., R. A. Locarnini, H. E. Garcia, T. D. O'Brien, T. P. Boyer, C. Stephens, and J. I. Antonov (2002), *World Ocean Atlas 2001: Objective Analyses, Data Statistics, and Figures* [CD-ROM] Natl. Oceanogr. Data Cent., Silver Spring, Md.

De Deckker, P., M. Moros, K. Perner, and E. Jansen (2012), Influence of the tropics and and southern westerlies on glacial interhemispheric asymmetry, *Nat. Geosci.*, *5*, 266–269, doi:10.1038/ngeo1431.

Eggins, S. M., A. Y. Sadekov, and P. De Deckker (2004), Modulation and daily banding of Mg/Ca in *Orbulina universa* tests by symbiont photosynthesis and respiration: A complication for seawater thermometry?, *Earth Planet. Sci. Lett.*, *225*, 411–419.

Elderfield, H., J. Yu, P. Anand, T. Kiefer, and B. Nyland (2006), Calibrations for benthic foraminiferal Mg/Ca paleothermometry and the carbonate ion hypothesis, *Earth Planet. Sci. Lett.*, *250*, 633–649.

Epstein, B. L., S. D'Hondt, J. G. Quinn, J. Zhang, and P. E. Hargraves (1998), An effect of dissolved nutrient concentrations on alkenone-based temperature estimates, *Paleoceanography*, *13*, 122–126.

Ferguson, J. E., G. M. Henderson, M. Kucera, and R. E. M. Rickaby (2008), Systematic change of foraminiferal Mg/Ca ratios across a strong salinity gradient, *Earth Planet. Sci. Lett.*, *265*(1–2), 153–166.

Fischer, G., and G. Wefer (1999), *Use of Proxies in Paleoceanography: Examples From the South Atlantic*, pp. 1–375, Springer, Berlin.

Gingele, F. X., and P. De Deckker (2005), Late Quaternary fluctuations of palaeoproductivity in the Murray canyons area, South Australian continental margin, *Palaeogeogr. Palaeoclimatol. Palaeoecol.*, *220*, 361–373.

Gingele, F. X., P. De Deckker, and C. D. Hillenbrand (2001), Late Quaternary fluctuations of the Leeuwin Current and palaeoclimates on the adjacent land masses: Clay mineral evidence, *Aust. J. Earth Sci.*, *48*, 867–874.

Gingele, F. X., P. De Deckker, and C.-D. Hillenbrand (2004), Late Quaternary terrigenous sediments from the Murray Canyons area, offshore South Australia and their implications for sea level change, palaeoclimate and palaeodrainage of the Murray-Darling Basin, *Mar. Geol.*, *212*, 183–197.

Gingele, F., P. De Deckker, and M. Norman (2007), Late Pleistocene and Holocene climate of SE Australia reconstructed from dust and river loads deposited offshore the River Murray Mouth, *Earth Planet. Sci. Lett.*, *255*, 257–272.

Gong, C., and D. J. Hollander (1999), Evidence for differential degradation of alkenones under contrasting bottom water oxygen conditions: Implications for paleotemperature reconstruction, *Geochim. Cosmochim. Acta*, *63*, 405–411.

Haarmann, T., E. C. Hathorne, M. Mohtadi, J. Groeneveld, M. Kölling, and T. Bickert (2011), Mg/Ca ratios of single planktonic foraminifer shells and the potential to reconstruct the thermal seasonality of the water column, *Paleoceanography*, *26*, PA3218, doi:10.1029/2010PA002091.

Herbert, T. D. (2003), Alkenones paleotemperature determinations, in *Treatise on Geochemistry*, vol. 6, *The Oceans and Marine Geochemistry*, pp. 391–432, Elsevier, Amsterdam.

Herfort, L., S. Schouten, J. P. Boon, and J. S. Sinninghe Damsté (2006), Application of the TEX_{86} temperature proxy to the southern North Sea, *Org. Geochem.*, *37*, 1715–1726.

Herndl, G. J., T. Reinthaler, E. Teira, H. van Aken, C. Veth, A. Pernthaler, and J. Pernthaler (2005), Contribution of *Archaea* to total prokaryotic production in the deep Atlantic Ocean, *Appl. Environ. Microbiol.*, *71*, 2303–2309.

Hill, P. J., and P. De Deckker (2004), AUSCAN seafloor mapping and geological sampling survey on the Australian southern margin by RV Marion Dufresne in 2003: Final project report, *Geosci. Aust. Rec.*, *2004/4*, 1–144.

Hoefs, M. J. L., G. J. M. Versteegh, W. I. C. Rijpstra, J. W. de Leeuw, and J. S. Sinninghe Damsté (1998), Postdepositional oxic degradation of alkenones: Implications for the measurement of palaeo sea surface temperatures, *Paleoceanography*, *13*, 42–49.

Hopmans, E. C., J. W. H. Weijers, E. Schefuß, L. Herfort, J. S. Sinninghe Damsté, and S. Schouten (2004), A novel proxy for terrestrial organic matter in sediments based on branched and isoprenoid tetraether lipids, *Earth Planet. Sci. Lett.*, *224*, 107–116.

Huguet, C., A. Schimmelmann, R. Thunell, L. J. Lourens, J. S. Sinninghe Damsté, and S. Schouten (2007), A study of the TEX_{86} paleothermometer in the water column and sediments of the Santa Barbara Basin, California, *Paleoceanography*, *22*, PA3203, doi:10.1029/2006PA001310.

Huguet, C., B. Martrat, J. O. Grimalt, J. S. Sinninghe Damsté, and S. Schouten (2011), Coherent millennial-scale patterns in $U^{K'}_{37}$ and TEX^{H}_{86} temperature records during the penultimate interglacial-to-glacial cycle in the western Mediterranean, *Paleoceanography*, *26*, PA2218, doi:10.1029/2010PA002048.

Hutson, W. H. (1977), Transfer-functions under no-analog conditions: Experiments with Indian Ocean planktonic foraminifera, *Quat. Res.*, *8*, 355–367.

Ikehara, M., K. Kawamura, N. Ohkouchi, K. Kimoto, M. Murayama, T. Nakamura, T. Oba, and A. Taira (1997), Alkenone sea surface temperature in the Southern Ocean for the last two deglaciations, *Geophys. Res. Lett.*, *24*, 679–682.

Imbrie, J., and N. G. Kipp (1971), A new micropaleontological method for quantitative paleoclimatology: Application to a late Pleistocene Caribbean core, in *The Late Cenozoic Glacial Ages*, pp. 71–181, Yale Univ. Press, New Haven, Conn.

Jouzel, J., et al. (2007), Orbital and millennial Antarctic climate variability over the past 800,000 years, *Science*, *317*, 793–796.

Karner, M. B., E. F. DeLong, and D. M. Karl (2001), Archaeal dominance in the mesopelagic zone of the Pacific Ocean, *Nature*, *409*, 507–510.

Kim, J.-H., X. Crosta, E. Michel, S. Schouten, J. Duprat, and J. S. Sinninghe Damsté (2009), Impact of lateral transport on organic proxies in the Southern Ocean, *Quat. Res.*, *71*, 246–250.

Kim, J.-H., J. van der Meer, S. Schouten, P. Helmke, V. Willmott, F. Sangiorgi, N. Koc, E. C. Hopmans, and J. S. Sinninghe Damsté (2010), New indices and calibrations derived from the distribution of crenarchaeal isoprenoid tetraether lipids: Implications for past sea surface temperature reconstructions, *Geochim. Cosmochim. Acta*, *74*, 4639–4654.

Kim, J.-H., O. E. Romero, G. Lohmann, B. Donner, T. Laepple, E. Haam, and J. S. Sinninghe Damsté (2012), Pronounced subsurface cooling of North Atlantic waters off Northwest Africa during Dansgaard-Oeschger interstadials, *Earth Planet. Sci. Lett.*, *339–340*, 95–102.

King, A. L., and W. H. Howard (2001), Seasonality of forminiferal flux in sediment traps at Chatham Rise, SW Pacific: Implications for paleotemperature estimates, *Deep Sea Res., Part I*, *48*, 1687–1708.

Könneke, M., A. E. Bernhard, J. R. de la Torre, C. B. Walker, J. B. Waterbury, and D. A. Stahl (2005), Isolation of an autotrophic ammonia-oxidizing marine archaeon, *Nature*, *437*, 543–546.

Lea, D., T. Mashiotta, and H. Spero (1999), Controls on magnesium and strontium uptake in planktonic foraminifera determined by live culturing, *Geochim. Cosmochim. Acta*, *63*, 2369–2379.

Lea, D. W., P. A. Martin, D. K. Pak, and H. J. Spero (2002), Reconstructing a 350 ky history of sea level using planktonic Mg/Ca and oxygen isotope records from a Cocos Ridge core, *Quat. Sci. Rev.*, *21*, 283–293.

Lee, K. E., J.-H. Kim, I. Wilke, P. Helmke, and S. Schouten (2008), A study of the alkenone, TEX_{86}, and planktonic foraminifera in the Benguela Upwelling System: Implications for past sea surface temperature estimates, *Geochem. Geophys. Geosyst.*, *9*, Q10019, doi:10.1029/2008GC002056.

Leider, A., K.-U. Hinrichs, G. Mollenhauer, and G. J. M. Versteegh (2010), Core-top calibration of the lipid-based $U^{K'}_{37}$ and TEX_{86} temperature proxies on the southern Italian shelf (SW Adriatic Sea, Gulf of Taranto), *Earth Planet. Sci. Lett.*, *300*, 112–124.

Li, Q., and B. McGowran (1998), Oceanographic implications of recent planktonic foraminifera along the southern Australian margin, *Mar. Freshwater Res.*, *49*, 439–445.

Li, Q., N. P. James, Y. Bone, and B. McGowran (1996), Foraminiferal biostratigraphy and depositional environments of the mid-Cenozoic Abrakurrie Limestone, Eucla Basin, southern Australia, *Aust. J. Earth Sci.*, *43*, 437–450.

Li, Q., P. J. Davies, and B. McGowran (1999), Foraminiferal sequence biostratigraphy of the Oligo-Miocene Janjukian strata from Torquay, southeastern Australia, *Aust. J. Earth Sci.*, *46*, 261–273.

Lisiecki, L. E., and M. E. Raymo (2005), A Pliocene-Pleistocene stack of 57 globally distributed benthic $\delta^{18}O$ records, *Paleoceanography*, *20*, PA1003, doi:10.1029/2004PA001071.

Locarnini, R. A., A. V. Mishonov, J. I. Antonov, T. P. Boyer, H. E. Garcia, O. K. Baranova, M. M. Zweng, and D. R. Johnson (2010), *World Ocean Atlas 2009, vol. 1, Temperature*, edited by S. Levitus, *NOAA Atlas NESDIS*, vol. 68, U.S. Gov. Print. Off., Washington, D. C.

Lopes dos Santos, R. A., M. Prange, I. S. Castañeda, E. Schefuß, S. Mulitza, M. Schulz, E. M. Niedermeyer, J. S. Sinninghe Damsté, and S. Schouten (2010), Glacial-interglacial variability in Atlantic meridional overturning circulation and thermocline adjustments in the tropical North Atlantic, *Earth Planet. Sci. Lett.*, *300*, 407–414.

Lopes dos Santos, R. A., D. Wilkins, P. De Deckker, and S. Schouten (2012), Late Quaternary productivity changes from offshore Southeastern Australia: A biomarker approach, *Palaeogeogr. Palaeoclimatol. Palaeoecol.*, *363–364*, 48–56.

Malmgren, B. A., and U. Nordlund (1997), Application of artificial neural networks to paleoceanographic data, *Palaeogeogr. Palaeoclimatol. Palaeoecol.*, *136*, 359–373.

Martinez, J. I., P. De Deckker, and T. T. Barrows (1999), Palaeoceanography of the last glacial maximum in the eastern Indian Ocean: Planktonic foraminiferal evidence, *Palaeogeogr. Palaeoclimatol. Palaeoecol.*, *147*, 73–99.

Menzel, D., E. C. Hopmans, S. Schouten, and J. S. Sinninghe Damsté (2006), Membrane tetraether lipids of planktonic Crenarchaeota in Pliocene sapropels of the eastern Mediterranean Sea, *Palaeogeogr. Palaeoclimatol. Palaeoecol.*, *239*, 1–15.

Mix, A. C. (1989), Influence of productivity variations on long-term atmospheric CO_2, *Nature*, *337*, 541–544.

Mohtadi, M., D. W. Oppo, A. Lückge, R. DePol-Holz, S. Steinke, J. Groeneveld, N. Hemme, and D. Hebbeln (2011), Reconstructing the thermal structure of the upper ocean: Insights from planktic foraminifera shell chemistry and alkenones in modern sediments of the tropical eastern Indian Ocean, *Paleoceanography*, *26*, PA3219, doi:10.1029/2011PA002132.

Moros, M., P. De Deckker, E. Jansen, K. Perner, and R. J. Telford (2009), Holocene climate variability in the Southern Ocean recorded in a deep-sea sediment core off South Australia, *Quat. Sci. Rev.*, *28*, 1932–1940.

Müller, P. J., G. Kirst, G. Ruhland, I. von Storch, and A. Rosell-Mele (1998), Calibration of the alkenone paleotemperature index ($U^{K'}_{37}$) based on core-tops from the eastern South Atlantic and the global ocean (60°N–60°S), *Geochim. Cosmochim. Acta*, *62*, 1757–1772.

Nodder, S. D., and L. C. Northcote (2001), Episodic particulate fluxes at southern temperate mid-latitudes (42–45°S) in the Subtropical Front region, east of New Zealand, *Deep Sea Res., Part I*, *48*, 833–864.

Nürnberg, D., and J. Groeneveld (2006), Pleistocene variability of the Subtropical Convergence at East Tasman Plateau: Evidence from planktonic foraminiferal Mg/Ca (ODP Site 1172A), *Geochem. Geophys. Geosyst.*, *7*, Q04P11, doi:10.1029/2005GC000984.

Nürnberg, D., J. Bijma, and C. Hemleben (1996), Assessing the reliability of magnesium in foraminiferal calcite as a proxy for water mass temperatures, *Geochim. Cosmochim. Acta*, *60*, 803–814.

Pahnke, K., and J. P. Sachs (2006), Sea surface temperatures of southern midlatitudes 0–160 kyr B.P., *Paleoceanography*, *21*, PA2003, doi:10.1029/2005PA001191.

Park, B.-J., S.-J. Park, D.-N. Yoon, S. Schouten, J. S. Sinninghe Damsté, and S.-K. Rhee (2010), Cultivation of autotrophic ammonia-oxidizing Archaea from marine sediments in coculture with sulfur-oxidizing bacteria, *Appl. Environ. Microbiol.*, *76*, 7575–7587.

Pearson, P. N., P. W. Ditchfield, J. Singano, K. G. Harcourt-Brown, C. J. Nicholas, R. K. Olsson, N. J. Shackleton, and M. A. Hall (2001), Warm tropical sea surface temperatures in the Late Cretaceous and Eocene epoch, *Nature*, *413*, 481–487.

Pelejero, C., E. Calvo, G. A. Logan, and P. De Deckker (2003), Marine isotopic stage 5e in the southwest Pacific: Similarities with Antarctica and ENSO inferences, *Geophys. Res. Lett.*, *30*(23), 2185, doi:10.1029/2003GL018191.

Pelejero, C., E. Calvo, T. T. Barrows, G. A. Logan, and P. De Deckker (2006), South Tasman Sea alkenone paleothermometry over the last four glacial/interglacial cycles, *Mar. Geol.*, *230*, 73–86.

Pflaumann, U., J. Duprat, C. Pujol, and L. D. Labeyrie (1996), SIMMAX: A modern analog technique to deduce Atlantic sea surface temperatures from planktonic foraminifera in deep-sea sediments, *Paleoceanography*, *11*, 15–35.

Pitcher, A., C. Wuchter, K. Siedenberg, S. Schouten, and J. S. Sinninghe Damsté (2011), Crenarchaeol tracks winter blooms of ammonia-oxidizing Thaumarchaeota in the coastal North Sea, *Limnol. Oceanogr.*, *56*, 2308–2318.

Prahl, F. G., and S. G. Wakeham (1987), Calibration of unsaturation patterns in long-chain ketone compositions for palaeotemperature assessment, *Nature*, *330*, 367–369.

Prahl, F. G., B. N. Popp, D. M. Karl, and M. A. Sparrow (2005), Ecology and biogeochemistry of alkenone production at station ALOHA, *Deep Sea Res., Part I*, *52*, 699–719.

Prahl, F. G., J.-F. Rontani, N. Zabeti, S. E. Walinsky, and M. A. Sparrow (2010), Systematic pattern in $U^{K'}_{37}$ - Temperature residuals for surface sediments from high latittude and other oceanographic settings, *Geochim. Cosmochim. Acta*, *74*, 131–143.

Rampen, S. W., V. Willmott, J.-H. Kim, E. Uliana, G. Mollenhauer, E. Schefuß, J. S. Sinninghe Damsté, and S. Schouten (2012), Long chain 1,13- and 1,15-diols as a potential proxy for palaeotemperature reconstruction, *Geochim. Cosmochim. Acta*, *84*, 204–216.

Ridgway, K. R., and S. A. Condie (2004), The 5500-km-long boundary flow off western and southern Australia, *J. Geophys. Res.*, *109*, C04017, doi:10.1029/2003JC001921.

Rommerskirchen, F., T. Condon, G. Mollenhauer, I. Dupont, and E. Schefuss (2011), Miocene to Pliocene development of surface and subsurface temperatures in the Benguela Current system, *Paleoceanography*, *26*, PA3216, doi:10.1029/2010PA002074.

Saito, T., R. R. Thompson, and D. Breger (1981), *Systematic Index of Recent and Pleistocene Planktonic Foraminifera*, Univ. of Tokyo Press, Tokyo.

Schouten, S., E. C. Hopmans, E. Schefuß, and J. S. Sinninghe Damsté (2002), Distributional variations in marine crenarchaeotal membrane lipids: A new tool for reconstructing ancient sea water temperatures?, *Earth Planet. Sci. Lett.*, *204*, 265–274.

Schouten, S., E. C. Hopmans, and J. S. Sinninghe Damsté (2004), The effect of maturity and depositional redox conditions on archaeal tetraether lipid palaeothermometry, *Org. Geochem.*, *35*, 567–571.

Schouten, S., A. Forster, F. E. Panoto, and J. S. Sinninghe Damsté (2007), Towards calibration of the TEX_{86} palaeothermometer for tropical sea surface temperatures in ancient greenhouse worlds, *Org. Geochem.*, *38*, 1537–1546.

Sikes, E. L., Howard, W. R., Neil, H. L., and J. K. Volkman (2002) Glacial-interglacial sea surface temperature changes across the subtropical front east of New Zealand based on alkenone unsaturation ratios and foraminiferal assemblages. *Paleoceanography*, *17*(2), 1012, doi:10.1029/2001PA000640.

Sikes, E. L., S. D. Nodder, T. O'Leary, and J. K. Volkman (2005), Alkenone temperature records and biomarker flux at the subtropical front on the Chatham Rise, SW Pacific, *Ocean, Deep Sea Res., Part I*, *52*, 721–748.

Sikes, E. L., W. R. Howard, C. R. Samson, T. S. Mahan, L. G. Robertson, and J. K. Volkman (2009), Southern Ocean seasonal temperature and Subtropical Front movement on the South Tasman Rise in the late Quaternary, *Paleoceanography*, *24*, PA2201, doi:10.1029/2008PA001659.

Sinninghe Damsté, J. S., W. I. C. Rijpstra, E. C. Hopmans, F. G. Prahl, S. G. Wakeham, and S. Schouten (2002), Distribution of membrane lipids of planktonic *Crenarchaeota* in the Arabian Sea, *Appl. Environ. Microbiol.*, *68*, 2997–3002.

Spero, H. J., J. Bijma, D. W. Lea, and B. E. Bemis (1997), Effect of seawater carbonate concentration on foraminiferal carbon and oxygen isotopes, *Nature*, *390*, 497–500.

Spooner, M. I., T. T. Barrows, P. De Deckker, and M. Paterne (2005), Palaeoceanography of the Banda Sea, and late Pleistocene initiation of the Northwest Monsoon, *Global Planet. Change*, *49*, 28–46.

Spooner, M. I., P. De Deckker, T. T. Barrows, and L. K. Fifield (2011), The behaviour of the Leeuwin Current offshore NW Australia during the last five glacial-interglacial cycles, *Global Planet. Change*, *75*, 119–132.

Ternois, Y., M.-A. Sicre, A. Boireau, M. H. Conte, and G. Eglinton (1997), Evaluation of long-chain alkenones as paleo-temperature indicators in the Mediterranean Sea, *Deep Sea Res., Part I*, *44*, 271–286.

Urey, H. C. (1947), The thermodynamic properties of isotopic substances, *J. Chem. Soc.*, *1947*, 562–581.

Volkman, J. K., S. M. Barrett, G. A. Dunstan, and S. W. Jeffrey (1992), C_{30}-C_{32} alkyl diols and unsaturated alcohols in microalgae of the class Eustigmatophyceae, *Org. Geochem.*, *18*, 131–138.

Waelbroeck, C., L. Labeyrie, J. C. Duplessy, J. Guiot, M. Labracherie, H. Leclaire, and J. Duprat (1998), Improving past sea surface temperature estimates based on planktonic fossil faunas, *Paleoceanography*, *13*, 272–283.

Weijers, J. W. H., S. Schouten, O. C. Spaargaren, and J. S. Sinninghe Damsté (2006), Occurrence and distribution of tetraether membrane lipids in soils: Implications for the use of the TEX_{86} proxy and the BIT index, *Org. Geochem.*, *37*, 1680–1693.

Wells, P., and H. Okada (1996), Holocene and Pleistocene glacial palaeoceanography off southeastern Australia, based on foraminifers and nannofossils in hole V18-222, *Aust. J. Earth Sci.*, *43*, 509–523.

Wells, P. E., and G. M. Wells (1994), Large-scale reorganization of ocean currents offshore western Australia during the late Quaternary, *Mar. Micropaleontol.*, *24*, 157–186.

Wilkins, D. (2009), Comparative optically stimulated luminescence (OSL) and AMS radiocarbon dating of Holocene lacustrine and marine deposits in southeast and southwestern Australia, *PhD thesis*, The Australian National University, Canberra, Australia.

Wuchter, C., et al. (2006), Archaeal nitrification in the ocean, *Proc. Natl. Acad. Sci. U. S. A.*, *103*, 12,317–12,322.